Rapid Publication

A ΔF508 Mutation in Mouse Cystic Fibrosis Transmembrane Conductance Regulator Results in a Temperature-sensitive Processing Defect In Vivo

Pim J. French,* J. Hikke van Doorninck,* Richard H.P.C. Peters,* Elly Verbeek,‡ Nadia A. Ameen,§ Christopher R. Marino,‖ Hugo R. de Jonge,¶ Jan Bijman,* and Bob J. Scholte*

*Departments of *Cell Biology, ‡Clinical Genetics and ¶Biochemistry, Erasmus University, 3000 DR Rotterdam, The Netherlands; §Department of Pediatric Gastroenterology, University of Miami, Florida 33136; and ‖Department of Medicine and Physiology, University of Tennessee, Memphis Tennessee 38163*

Abstract

The most prevalent mutation (ΔF508) in cystic fibrosis patients inhibits maturation and transfer to the plasma membrane of the mutant cystic fibrosis transmembrane conductance regulator (CFTR). We have analyzed the properties of a ΔF508 CFTR mouse model, which we described recently. We show that the mRNA levels of mutant CFTR are normal in all tissues examined. Therefore the reduced mRNA levels reported in two similar models may be related to their intronic transcription units. Maturation of mutant CFTR was greatly reduced in freshly excised oviduct, compared with normal. Accumulation of mutant CFTR antigen in the apical region of jejunum crypt enterocytes was not observed, in contrast to normal mice. In cultured gallbladder epithelial cells from ΔF508 mice, CFTR chloride channel activity could be detected at only two percent of the normal frequency. However, in mutant cells that were grown at reduced temperature the channel frequency increased to over sixteen percent of the normal level at that temperature. The biophysical characteristics of the mutant channel were not significantly different from normal. In homozygous ΔF508 mice we did not observe a significant effect of genetic background on the level of residual chloride channel activity, as determined by the size of the forskolin response in Ussing chamber experiments. Our data show that like its human homologue, mouse ΔF508-CFTR is a temperature sensitive processing mutant. The ΔF508 mouse is therefore a valid in vivo model of human ΔF508-CFTR. It may help us to elucidate the processing pathways of complex membrane proteins. Moreover, it may facilitate the discovery of new approaches towards therapy of cystic fibrosis. (*J. Clin. Invest.* 1996. 98:1304–1312.) Key words: cystic fibrosis • chloride channel • antibody • animal models • patch clamp

Address correspondence to Dr. Bob J. Scholte, Cell Biology, Erasmus University, P.O. Box 1738, 3000 DR Rotterdam, The Netherlands. Phone: 10 408 7205; FAX: 10 436 0225; E-mail: scholte@ch1.fgg.eur.nl

Introduction

Cystic fibrosis is the most common lethal genetic disease in the Caucasian population (1, 2). It is caused by mutations in the gene encoding the cystic fibrosis transmembrane conductance regulator (CFTR)[1] (3). CFTR is a cAMP-regulated chloride channel, which is expressed in the apical membrane of many epithelia. The most common mutation in cystic fibrosis (CF) patients is a deletion of a phenylalanine at position 508 (ΔF508) (4). This mutation affects correct processing of the protein to its mature, fully glycosylated form (5, 6). The ΔF508 form of CFTR is retained in the endoplasmic reticulum and degraded, and does not reach the apical plasma membrane (7, 8). However, ΔF508-CFTR can function as a cAMP regulated chloride channel, both in the endoplasmic reticulum (9) and when expressed on the apical plasma membrane. The latter occurs when ΔF508-CFTR expressing cells are cultured at low temperatures (10) and when Vaccinia expression vectors are used (11). Cells cultured at lower temperatures, Sf9 insect cells (12) and *Xenopus* oocytes (13), also express functional ΔF508-CFTR on the plasma membrane when transduced with a ΔF508-CFTR expression vector. The clinical significance of this observation is that it may lead to a new approach towards the therapy of CF based on relieving the processing defect. In an attempt to facilitate research in this field we have recently reported the generation of a mouse model with the ΔF508-CFTR mutation using the "hit and run" mutagenesis procedure (14). In this model the intron structure is not disturbed in contrast to two similar models presented (15, 16). In our previous studies we demonstrated severely reduced chloride permeability in several epithelial tissues, confirming a CF phenotype. However, in Ussing chamber experiments with intact gall bladder and intestinal tissue from mutant mice we observed a small residual cAMP regulated chloride secretion, possibly due to the presence of some functional ΔF508-CFTR (14). Our present study shows that the mouse ΔF508-CFTR is not processed efficiently to the fully glycosylated form in vivo. However, the mutant protein is expressed as functional chloride channels in the plasma membrane of cells cultured at reduced temperature. Furthermore, we could show that the electrophysiological characteristics of the mouse ΔF508-CFTR channels were indistinguishable from normal.

---

1. *Abbreviations used in this paper:* CF, cystic fibrosis; CFTR, cystic fibrosis transmembrane conductance regulator.

Methods

Animals. All animal experiments were performed according to the guidelines issued by the Dutch government concerning animal care. Mice with the ΔF508 mutation were described by Van Doorninck et al. (14). Mice with a targeted disruption in the CFTR gene (cftr^m1cam knockout mice, CF−/−) resulting in complete loss of function were obtained from Ratcliff et al. (17). All animals were bred under pathogen-free conditions in our transgenic unit. The genotype of each individual animal was tested by Southern blotting of tail DNA. The CF−/− animals in our facility display less severe runting and lower mortality due to intestinal obstruction as reported for the Cambridge colony, which may be due to breeding conditions. All physiological parameters measured, nasal potential differences (PD), intestinal and gall bladder PD measurements (14, 17a), confirmed the CF−/− phenotype of these animals. The animals used for the experiments reported here were 5–6 wk old, without obvious signs of disease or discomfort, with an average weight of 23 ± 3 grams. All experiments involving ΔF508 mice were performed with the strain in 129/FVB genetic background (14) using littermates as control in parallel experiments. The experiments presented in Fig. 7 were performed with three different ΔF508 CFTR mouse colonies as described in text.

Quantitative PCR analysis. Two mouse specific oligonucleotides MCF2 (5′-AATGACCACAGGCATAATC-3′), and MCF3 (5′-CAA-CACTCTTATATCTGTAC-3′) were synthesized. The sequences are localized in exons 8 and 10, respectively, and generate a mouse CFTR mRNA-specific 403-bp fragment in RT-PCR analysis. Total RNA was isolated by extraction of various mouse tissues or cultured cells in guanidine isothiocyanate and centrifugation through a 5.2 mol/liter CsCl step-gradient. The RNA was reversed transcribed to cDNA by adding 10 U Avian myoblastoma virus reverse transcriptase (AMV-RT) in 20 μl cDNA buffer (7 μg heat denatured RNA, 0.8 μmol/liter antisense oligonucleotide primer MCF3), 10^{-3} mol/liter dNTP's, 0.05 mol/liter KCl, 0.02 mol/liter Tris-HCl pH 8.4, 0.0025 mol/liter MgCl₂, 0.1 grams/liter bovine serum albumin and 20 U of RNasin for 1 h at 37°C. The 50 μl PCR assay contained $0.3 \cdot 10^{-6}$ mol/liter sense and antisense oligonucleotide primer (MCF2 and MCF3, $0.2 \cdot 10^{-3}$ mol/liter dNTP's, 4 μl cDNA mix, 0.05 mol/liter KCl, 0.02 mol/liter Tris-HCl ph 8.4, $2.5 \cdot 10^{-3}$ mol/liter MgCl₂, and 0.1 grams/liter bovine serum albumin. After denaturing at 94°C, 5 U Taq polymerase was added at 72°C. Standard cycling program: 30 cycles of denaturation for 2 min at 93°C, primer annealing for 2 min at 47°C, and elongation for 4 min at 72°C. Aldolase A oligonucleotide primers, which amplify a 442-bp cDNA fragment, were as in Bremer et al. (18). To check the quality of the RNA and the PCR procedure, the amplification of aldolase A sequences was done in parallel, under the same conditions as described above for CFTR. PCR products were separated on a 1.5% agarose gel. For quantitative analysis of the PCR reaction, equal amounts of total RNA isolated from different tissues were subjected to an RT-PCR protocol in parallel incubations. Aliquots were withdrawn at regular intervals from the PCR and subjected to Southern blotting. Radioactivity was measured with a Phosphorimager (Molecular Dynamics, Inc., Sunnyvale, CA).

Western blot analysis of oviduct. Female mice of different phenotypes were anesthetized with ether. The lower abdomen was opened and the oviducts were dissected. After rapid excision the oviducts from one mouse were pooled and immediately solubilized by vortexing followed by brief sonication in 30 μl of modified Laemmli sample buffer (Tris-HCl 0.06 mol/liter, 2% (wt/vol) SDS, 15% (wt/vol) Glycerol, 2% (vol/vol) β-mercaptoethanol, 0.05 grams/liter leupeptin, 0.05 grams/liter soybean trypsin inhibitor, 0.03 grams/liter phosphoramidon, 10^{-4} mol/liter Pefabloc (Boehringer Mannheim, Mannheim, Germany), 10^{-3} mol/liter benzamidine, 0.1% (wt/vol) bromophenol-blue, pH 6.8). The samples were incubated for ten minutes at 37°C and centrifuged (2 min, 8,000 *g*). Samples of the supernatants (10 μl, containing about 20 μg protein) were separated on 6% poly-acrylamide slabgels using a Bio-Rad Miniprotean apparatus (Bio-Rad Laboratories, Herfordshire, UK). Proteins were subsequently electro-

blotted onto nitrocellulose paper (0.1 μm pore size, Schleicher and Schuell, Inc., Keene, NH) in 0.025 mol/liter Tris, 0.192 mol/liter glycine, 20% (vol/vol) methanol. The blots were then incubated overnight at 4°C with 0.02 mol/liter Tris-HCl, 0.5 mol/liter NaCl, 0.05% (wt/vol) Tween20 (TTBS), followed by an overnight incubation at 4°C with a 1:3000 dilution of affinity purified antibody R3195 in TTBS. The blots were washed three times in TTBS, incubated with peroxidase conjugated anti–rabbit IgG (Tago Inc., Burlingame, CA; 1:3000 in TTBS for 2 h), and washed four times with TTBS. Peroxidase activity was detected with bioluminescence reagents (Amersham, Braunschweig, Germany) on x-ray film. The rabbit polyclonal antibody R3195 was developed against the 13–amino acid COOH-terminal peptide sequence of rodent CFTR, conjugated to bovine thyroglobulin. The antibody was affinity-purified on a peptide-epoxide activated Sepharose column, eluted with 4.9 mol/liter MgCl₂, dialyzed and concentrated.

Immunocytochemistry. Non-fasted mice were killed after inhalation anaesthesia. Intestinal tissues were quickly removed and frozen in OCT embedding medium (Miles Lab., Elkhardt, In.) using liquid nitrogen cooled 2-methylbutane. Cryosections (5 μm) were fixed with 3% (wt/vol) paraformaldehyde (10 min) and methanol (20 min), washed with phosphate-buffered saline supplemented with 1% bovine serum albumin and protease inhibitors before incubation with the anti CFTR antibody R3195 (1/500). Antibody labelling was detected with FITC conjugated anti–rabbit F(ab)2 fragments (Boehringer, Mannheim, Germany).

Gall bladder epithelial cell culture. Gall bladders were removed from the animal. After the bile was washed out with RPMI-1640 medium supplemented with 100 U/ml penicillin, 0.1 grams/liter streptomycin, and 0.02 mol/liter Hepes pH 7.2, the gallbladders were cut into small pieces and embedded in 1 mm collagen gels (Sigma Chemical Co., St. Louis. MO; Calf skin type I). The explant cultures were incubated at 37 °C in a humidified 10% CO₂/air mixture in Dulbecco's Modified Eagle's Medium (DME) supplemented with 100 U/ml penicillin, 0.1 grams/liter streptomycin, 0.002 mol/liter glutamine, and 10% fetal calf serum. Mouse gall bladder epithelial cells could be cultured for up to 3 wk, with medium changes every 2–3 d.

Patch clamp analysis. Patch clamp experiments, data sampling and analysis were performed as previously described (19). Patch pipettes, borosilicate glass (Clark GC150-TF) were pulled to a resistance of 3-8 MOhm. Excised patches were transferred to a solution exchange compartment (19). This allowed us to add various substrates (ATP, protein kinase A) and to change the buffer composition to a I⁻, F⁻, NO3⁻, Br⁻, or gluconate buffer. Pipette (external) and bath (internal) solutions contained (mol/liter) 0.14 NaCl, $5 \cdot 10^{-3}$ KCl, $1.2 \cdot 10^{-3}$ MgCl₂, $0.15 \cdot 10^{-3}$ CaCl₂, 10^{-3} EGTA, and $5 \cdot 10^{-3}$ Hepes. Final Ca²⁺ concentration was 10^{-8} M, pH 7.4. Low chloride buffer was identical except that it contained 0.14 mol/liter Na-gluconate instead of NaCl, except for the low chloride pipet buffer used to analyzes normal mouse CFTR. This buffer contained (mol/liter) 0.140 N-methyl-d-glucamine (NMDG), $5 \cdot 10^{-3}$ CaCl₂, $2 \cdot 10^{-3}$ MgCl₂, 10^{-2} Hepes and 0.1 D-Aspartic acid adjusted to pH 7.2, final chloride concentration $49 \cdot 10^{-3}$. High (0.427 mol/liter) chloride buffers contained 0.420 mol/liter NaCl. In other buffers 0.140 mol/liter NaCl was replaced with either NaI, NaBr, NaNO₃, NaF, or Na-Gluconate, all 0.140 mol/liter. All experiments were performed at 37°C. A List LM-EPC 7 (Darmstadt, Germany) amplifier was used for current amplification and voltage clamping. Data were digitalized (Sony PCM-F1) and stored on videotape. For analysis, data were filtered at 50 Hz, sample frequency 100 Hz, and transferred to a personal computer (Tulip 386sx). Pipette potential refers to the voltage applied to the pipette interior with respect to the (grounded) bath. Positive (upward) currents represent negative charge flowing out of the pipette. $V_{I=0}$ was corrected for the liquid junction potential. Experiments presented in Fig. 6 were performed blinded with respect to the genotype of the cells under study.

Ussing chamber experiments. Mouse gallbladder and caecum were mounted in an Ussing chamber, basal electric potential and re-
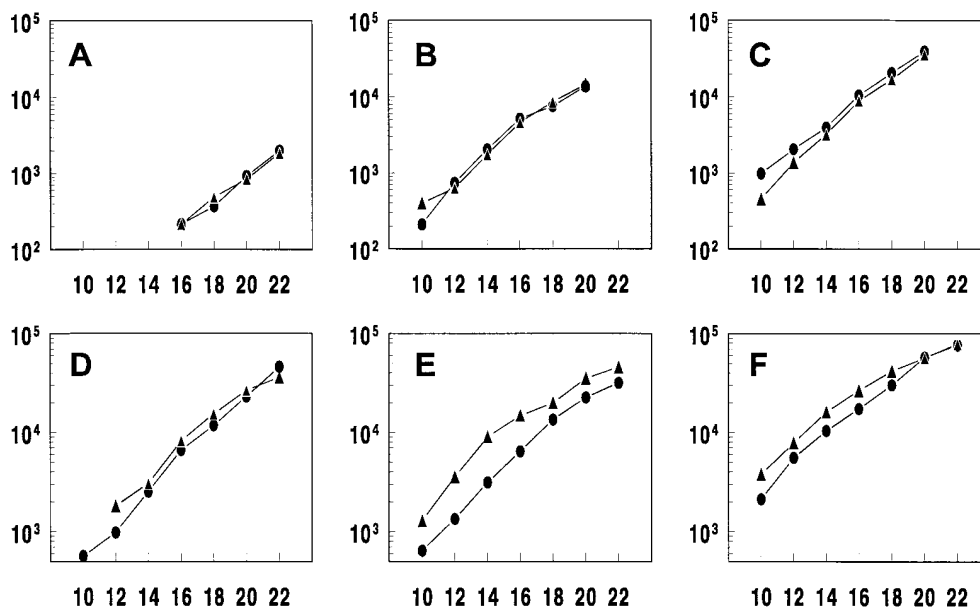
Figure 1. Quantitative analysis of CFTR mRNA expression. Total RNA from normal and mutant mice was isolated from different tissues and subjected to RT-PCR analysis in parallel experiments as described. Specific primers in mouse *Cftr* exons 8 and 10 yielded a 403-bp fragment, which contained an SspI site only when the product was initiated on a ΔF508-CFTR mRNA (14). Samples collected at different cycle intervals were subjected to Southern blotting using the labeled 403-bp fragment as a probe. Data shown here represent the amount of radioactivity per band in arbitrary units. Data from different panels are not corrected for differences in blotting efficiency. PCR products from heterozygous mice (ΔF/+) were digested with SspI before Southern analysis (*A–C*). Data indicate the amount of PCR product from the normal allele (403 bp, ●–●) and from the ΔF508 allele (359 bp, ▲–▲) when RNA was isolated from salivary gland (*A*), caecum (*B*), and jejunum (*C*) of heterozygous mice. PCR products from homozygous normal (●–●) and homozygous ΔF508 mice (▲–▲) were compared in parallel, using RNA isolated from salivary gland (*D*), caecum (*E*), and jejunum (*F*). The data show that there is no significant difference in the levels of mutant and normal CFTR mRNA. RNA from CFTR knockout mice (17) did not produce a PCR product in a parallel experiment whereas the aldolase primers produced comparable amounts of PCR product in all samples tested (not shown).

sponses to forskolin (10^{-5} mol/liter) were determined as described by van Doorninck et al. (14).

Statistical analysis. Significance analysis was tested with linear regression analysis for the current-voltage data presented in Fig. 5, and with a Student's *t* test (unequal variance) for the channel frequency determination (Fig. 6)

Results

ΔF508 mice have normal CFTR mRNA levels. The ΔF508 mouse model from our laboratory was generated by the "hit and run" procedure. With this method the mutation is introduced in an otherwise normal mouse *cftr* gene. Therefore, CFTR mRNA transcription and processing rates are expected to be normal. This is particularly important as low ΔF508-CFTR mRNA levels were reported in tissues of two other ΔF508-CFTR mouse models which were made while introducing a selectable marker in the intron structure (15,16). To investigate this we have performed quantitative RT-PCR analysis with RNA isolated from heterozygous and homozygous ΔF508 mice. As controls we have used normal littermates and homozygous *cftr* knockout mice (17). The PCR product from the mutant allele contains an SspI restriction site which is not present in the wild type allele (14). This allowed us to accurately determine the ratio of normal and mutant CFTR mRNA in a single PCR experiment with RNA from a heterozygous animal. With this approach we can rule out variations introduced by differences in reaction conditions and quality of RNA preparations. Our data show that the steady state levels of normal and ΔF508-CFTR mRNA are virtually identical in different regions of the intestine and in salivary gland (Fig. 1, *A–C*). Therefore, the mutation that we have introduced does not significantly affect mRNA synthesis processing or stability in epithelial tissues. In

experiments with RNA isolated from homozygous animals ΔF508-CFTR, mRNA levels did not differ significantly from normal values (Fig. 1, *D–F*). This confirms that also in homozygous deficient animals expression of the gene in these tissues is not reduced.

Abnormal processing of ΔF508-CFTR in mouse oviduct. Western blot analysis (N = 3) of mouse CFTR from normal oviduct (Fig. 2, +/+) showed the characteristic pattern as observed for human CFTR, a core-glycosylated form (band *B*)
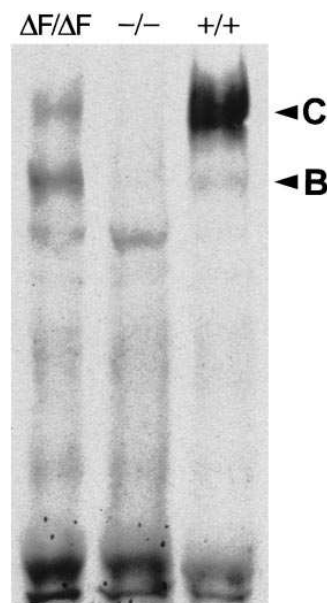
Figure 2. CFTR in mouse oviduct. Oviduct from normal (+/+), homozygous ΔF508 (ΔF/ΔF), and CFTR deficient (−/−) mice were subjected to Western blot analysis as described in the methods section. *C* indicates the fully glycosylated form of mouse CFTR antigen, *B* indicates the core-glycosylated precursor. The data show that ΔF508-CFTR is not glycosylated to the same extent as the normal form.
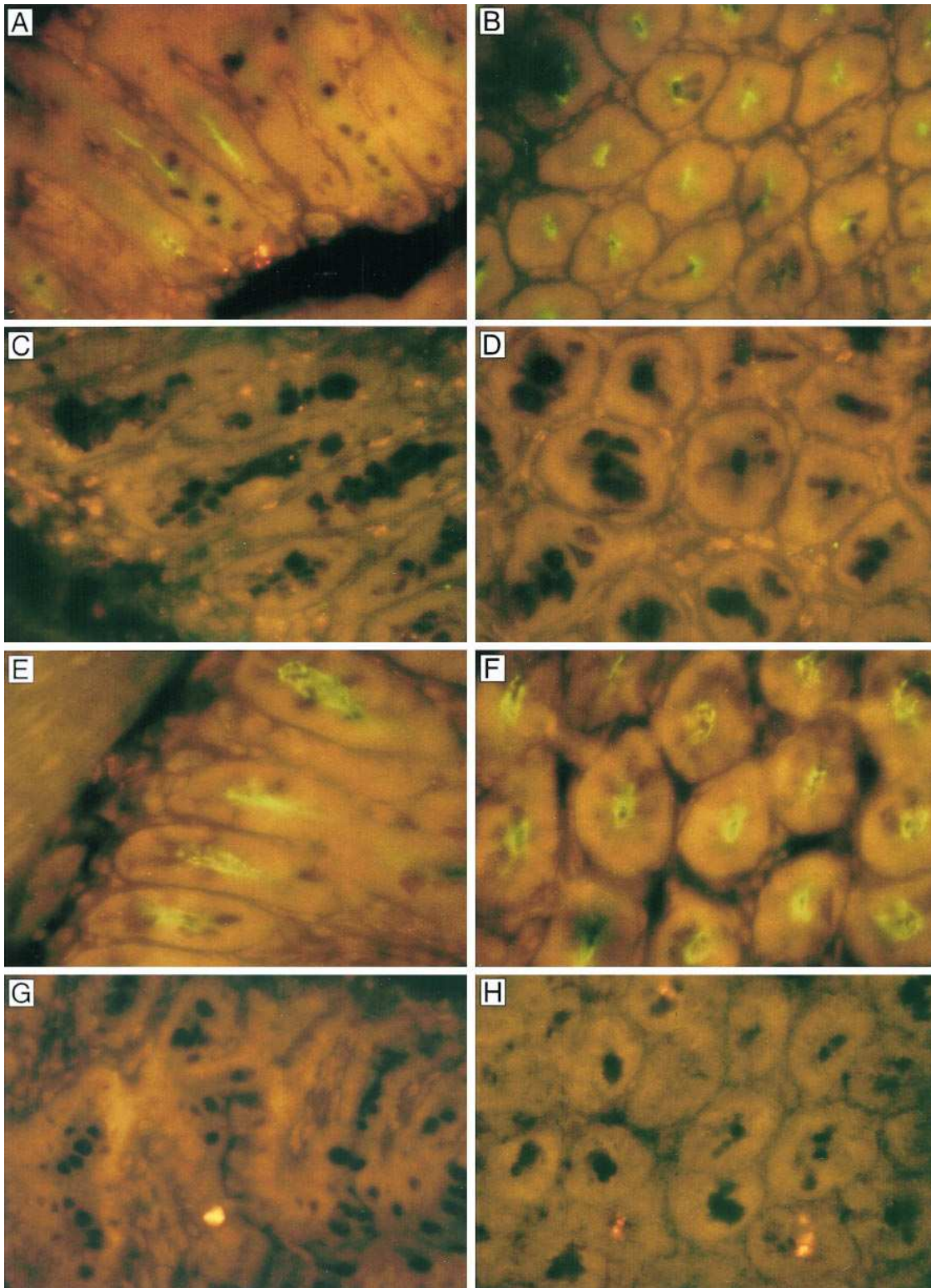
Figure 3. CFTR in mouse jejunum. Immunocytochemical detection of CFTR antigen in jejunal crypts from normal (*A* and *B*, +/+ cftr^{m1cam} colony; *E* and *F*, +/+ ΔF508cftr colony), CFTR deficient (−/− cftr^{m1cam}) mice (*C* and *D*), and homozygous ΔF508 mice (*G* and *H*), and was performed as described in the methods section, using a polyclonal antibody against the murine CFTR carboxy terminal. Normal crypts show intense staining of the apical region of the epithelial cells. This is not observed with crypts from CFTR −/− mice or in ΔF/ΔF mice.

and forms containing complex N-linked oligosaccharides (band C) (3). In oviduct from a mouse with a complete loss of function mutation (Fig. 2, −/−) (17) these bands were not observed. Oviduct from a homozygous ΔF508 mouse (Fig. 2, ΔF/ΔF) produced a prominent band B and some band C antigen. The ratio of B over C is increased over 50-fold compared with the normal ratio as estimated by scanning the original radiograph. This strongly suggests that processing and subsequent glycosylation of mouse ΔF508 CFTR is severely affected in this tissue, as described previously for the human form of ΔF508 CFTR (5, 6). Gallbladder, pancreas and intestine did not give reproducible data with this technique.

Mouse ΔF508-CFTR is not efficiently transported to the apical membrane. Immunocytochemical detection of CFTR antigen in normal jejunal crypt shows intense staining of the apical region of all crypts (N = 7, Fig. 3 *A, B* and *E, F*). This is in accordance with immunocytochemical localization studies published previously for human intestine (20). In jejunal crypts from mice with a loss of function mutation (17), no CFTR-specific apical staining is observed (N = 6, Fig. 3, *C* and *D*). This confirms the specificity of the staining. Jejunum crypts of homozygous ΔF508 mice generally showed no clear apical CFTR antigen (N = 6, Fig. 3, *G* and *H*). In some preparations (three out of six) a diffuse cytoplasmic stain was observed in the epithelial crypt cells. The immunocytochemical method used here

is characterized by an inherently nonlinear relationship between signal intensity and local antigen density. Moreover the absolute level of staining intensity varies per experiment. Therefore we can neither quantitate the level of correct processing nor the level of antigen expression in homozygous ΔF508 mice with any accuracy. The data presented show that despite the normal CFTR mRNA levels in ΔF/ΔF mice (Fig. 1) the amount of apical CFTR antigen in the jejunum crypt is greatly reduced. This is in agreement with our functional studies in intestinal tissue of mouse (14) and human (21) ΔF508-CFTR mutants. Moreover, it is in agreement with immunocytochemical studies in airway cells (22) and in cell culture (23). Other tissues that we have tested for CFTR specific staining with this method (gallbladder, cystic duct, pancreas) did not show consistent specific staining above background signals observed in tissues from knockout mice.

Patch clamp analysis of mouse ΔF508-CFTR. CFTR mRNA is expressed in mouse gallbladder epithelial cells, both in situ and in primary culture (17a). We have determined the number and properties of normal and ΔF508-CFTR chloride channels by patch clamp analysis of mouse gallbladder epithelial cells in primary culture. In excised membrane patches from unstimulated normal (+/+ and +/ΔF) cells, a linear 5.1±0.1 pS (SE) could be activated by the addition of protein kinase A in the presence of ATP (Fig. 4 *A*). In cell attached membrane
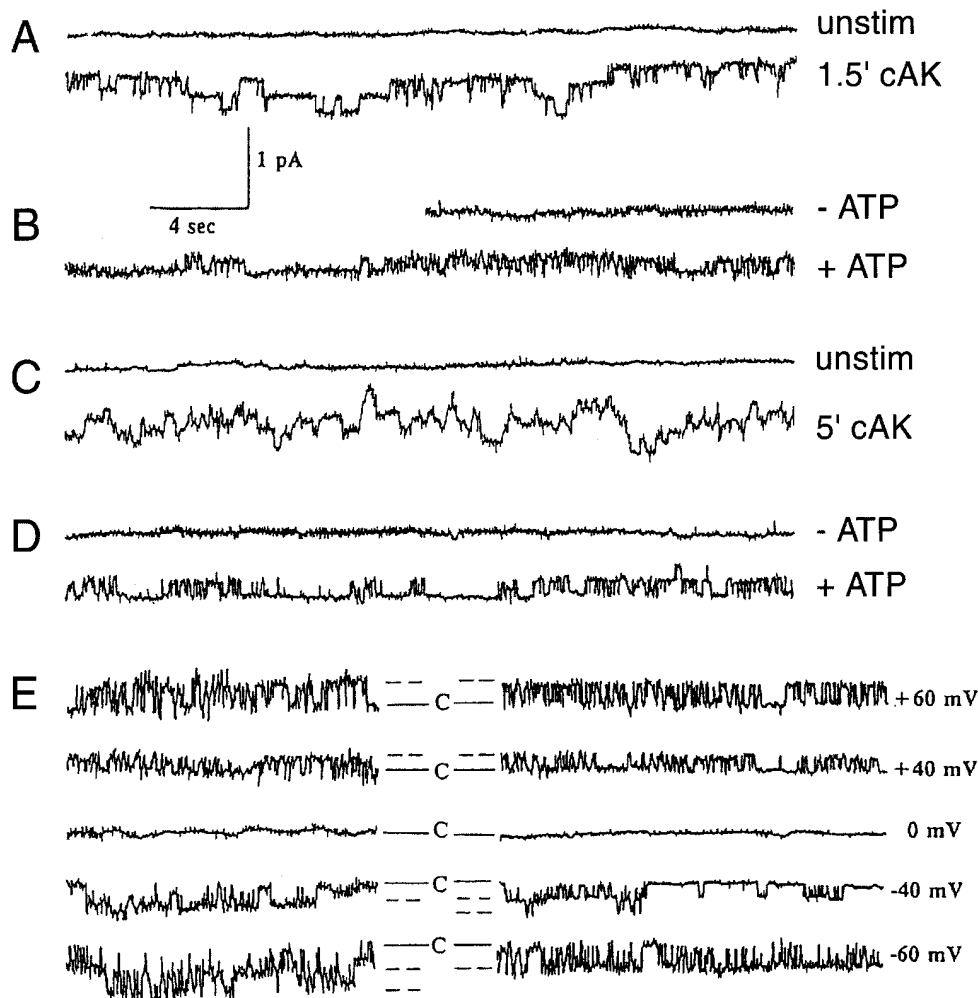

Figure 4. Characterization of normal and ΔF508 CFTR chloride channel activity. Current tracings of CFTR activity in excised patches from normal (*A* and *B*) and ΔF508 (*C* and *D*) mouse gallbladder epithelial cells cultured at 27°C. Unstimulated excised, inside-out patches from cultured gallbladder epithelial cells generally showed no channel activity. Upon a short incubation with the catalytic subunit of protein kinase A (cAK, 2 mU/ml) in the presence of 2.10^{-3} mol/liter ATP, a low conductance channel was observed in both normal and ΔF508 cells (*A* resp. *C*). Active patches of forskolin stimulated cells became silent upon excision (*B* and *D*, −ATP), but could be reactivated by the addition of 2.10^{-3} mol/liter ATP alone both in normal (*B*) and ΔF508 CFTR (*D*, +ATP). (*E*) Current tracings at different holding potentials from normal (*left tracings*) and ΔF508 CFTR (*right tracings*). Holding potential was +40 mV scale bar as indicated, except for *C* where the holding potential was + 60 mV, scale bar 4 s, 1.5 pA.

patches of forskolin-stimulated normal cells channels were observed at an average of 27.6±16.5 (SEM) per patch (Fig. 6 *left*). Excision of the membrane inactivated the channel but it could be reopened by addition of ATP (Fig. 4 *B*). Considering the resemblance with human CFTR (3) we conclude that these linear chloride channels represent normal mouse CFTR. The only difference observed between mouse and human CFTR is the lower conductance of the channel (human CFTR 8.0±0.6 pS) (3). In homozygous mutant cells cultured at 37°C the number of functional CFTR channels per patch is about 1% of normal (+/+ and +/ΔF, $P < 0.02$) (Fig. 6), but not zero. These data confirm our conclusion that the expression of CFTR activity on the plasma membrane of homozygous mutant cells is greatly reduced but not completely absent (14). In cells expressing human ΔF508-CFTR an increase of apical channel activity has been observed when cells were grown at reduced temperature, which is associated with a conversion of core-to-complex chain glycosylation and increased apical localization of ΔF508-CFTR (10). In normal (+/+) and heterozygote (ΔF/+) mouse gall bladder cells grown at 27°C for 3–7 d we observed a twofold decrease in CFTR channel frequency compared to 37°C (Fig. 6). In contrast, ΔF/ΔF cells cultured at 27°C show a considerable increase in ΔF508-CFTR channel frequency compared to cells cultured at 37°C ($P < 0.05$). The average number of channels per patch was 16% of the average observed in normal cells cultured at 27°C (Fig. 6). The high frequency at which the ΔF508-CFTR channel was observed in cells cultured at lower temperatures enabled us to study its properties in detail. ΔF508-CFTR could be observed in cell attached patches after addition of forskolin. The channel became silent upon excision but could be reactivated by the addi-

tion of ATP (Fig. 4 *D*). Excised membrane patches from unstimulated ΔF/ΔF cells were silent, but CFTR-like channel activity was observed by the addition of protein kinase A plus ATP (Fig. 4 *C*). These data show that mouse ΔF508-CFTR has a normal protein kinase and ATP regulation. Mouse ΔF508-CFTR is a linear 4.9±0.1 pS chloride channel, similar to normal mouse CFTR, 5.1±0.1 (SE) (Fig. 5, *A–B*). Lowering or increasing the chloride concentration in the bath results in a shift in the reversal potential ($V_{I=0}$), indicative for anion selectivity (Fig. 5, *A–B*). The relative cation to anion permeability, $P_{cat}/P_{Cl} = 0.14$ and 0.16 for normal and ΔF508-CFTR respectively (calculated from the least permeant anion, i.e., F^-). When chloride was substituted for other monovalent anions the relative permeability was determined as $NO_3^- > Br^- > Cl^- >> $ gluconate $> F^-$ for both normal (Fig. 5 *C*) and ΔF508-CFTR (Fig. 5 *D*). Iodine had a high affinity but low permeability for both normal and ΔF508-CFTR (Fig. 5, *C* and *D*) which is a characteristic for CFTR (3). The open probability (Po) of ΔF508-CFTR (0.33±0.04) is comparable with normal mouse CFTR (0.35±0.04) ($n = 5$, values±SE, excised patches from forskolin activated cells in the presence of ATP). The Po of both normal and mutant CFTR was voltage independent. Channel "flickering," i.e., the number of closing events during a period of activation, also did not differ significantly between ΔF/ΔF (3.99±0.70 s⁻¹, $n = 12$) and normal (+/+) cells (3.23±0.55 s⁻¹, $n = 7$ patches, ±SE). We conclude that, similar to human ΔF508-CFTR, trafficking of the mouse ΔF508-CFTR to the plasma membrane is greatly increased at reduced temperature. Moreover, the biophysical properties of the mouse ΔF508-CFTR channel do not differ significantly from the wild type form.
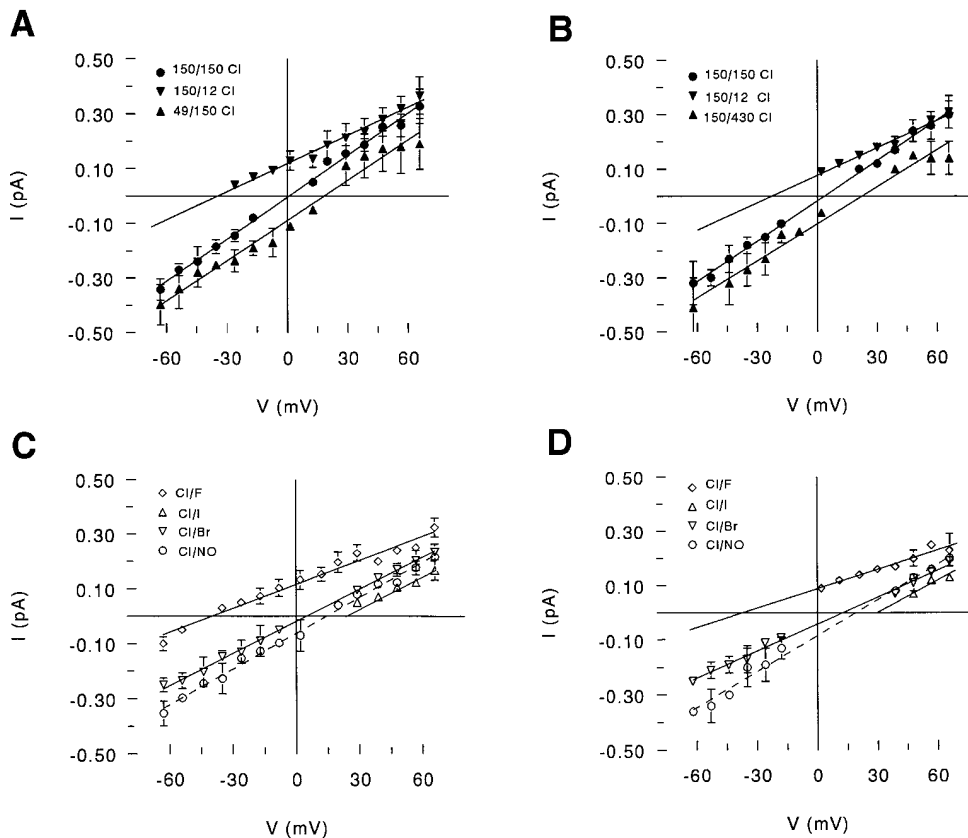
*Figure 5.* Current-voltage characteristics and relative anion permeability of normal and ΔF508 mouse CFTR. Current-voltage relationships of normal (*A* and *C*) and ΔF508-CFTR (*B* and *D*). At equal pipet and bath chloride concentrations (●-●, 0.150 mol/liter) both normal and ΔF508-CFTR show a linear conductance of 5.1±0.1 resp. 4.9±0.1 pS. A shift in the reversal potential ($V_{I=0}$) expected for a chloride channel was observed when bath chloride concentration was higher (▲-▲) or lower (▼-▼) than the pipet concentration (*A* and *B*). By replacing chloride in the bath with other anions as indicated (*C* and *D*), the relative ion selectivity was determined as $NO_3^- > Br^- > Cl^- >> $ gluconate $> F^-$ for both normal (*C*) and ΔF508-CFTR (*D*). Iodine has a high affinity but low permeability in both normal and ΔF508-CFTR, as in human CFTR.
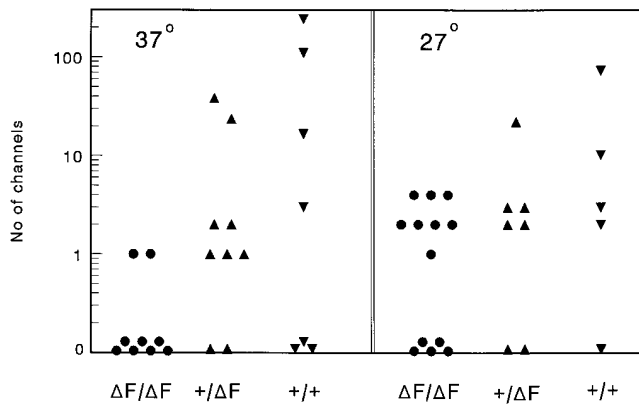
Figure 6. CFTR chloride channels in gall bladder plasma membrane. CFTR channel activity on plasma membrane of cultured gallbladder epithelial cells was recorded with patch clamp analysis as described. Cells were cultured either at 37°C (*left*) or at 27°C (*right*) for 3–7 d before analysis. Forskolin stimulated cells were recorded for two minutes in the on cell patch clamp configuration, followed by a 1–10-min recording in the excised patch configuration in the presence of 2 mM ATP. CFTR channel frequency was calculated from the equation $n = I_a/(I_1 \cdot Po)$ where n is the calculated number of levels, I_a is the average current in the patch, I_1 is the current of one channel at holding potential, and Po is the open probability. When 4 or less levels of activity were observed in the patch the equation was not used, in these cases the number of channels correspond directly to the number of current levels observed. Patches which showed no CFTR activity were scored as zero. Cells were obtained from parallel cultures of littermates. (●) Homozygous mutant, ΔF/ΔF (cells from 3 mice at 37°C and 8 mice at 27°C); (▲) heterozygous mutant +/ΔF (3 and 4 mice); (▼) homozygous normal +/+ mice (2 and 1 mice).

Inefficient processing of mouse ΔF508 CFTR is observed in different genetic backgrounds. The most sensitive available measure of apical CFTR activity is probably the steady state response to forskolin in Ussing chamber experiments. Using this method, we have previously shown low but significant residual ΔF508-CFTR activity in different tissues of homozygous ΔF508 mice when compared to cftr[m1cam] knockout mice that showed no activity (14). Next, we studied whether genetic background influences the level of ΔF508-CFTR processing. The 129*FVB and 129*C57Bl/6 ΔF strains were obtained by introduction of the original mutant clone (129/Ola) in FVB and C57BL/6 blastocysts respectively, ΔF/+ (129*FVB) mice were crossed with cftr[m1cam] knockout mice (KO) that are 129*C57BL/6. The forskolin response of gallbladder and caecum of these different ΔF mouse strains was monitored in Ussing chamber experiments. For all strains the forskolin response was equally reduced in homozygous ΔF/ΔF and in ΔF/− mice (Fig. 7). All individual measurements from ΔF mutant mice are in the same range with only one exception observed (Fig. 7). The data show no evidence for dominant alleles in either the 129/Ola, FVB or C57BL/6 inbred genetic backgrounds that significantly increase or reduce the level of ΔF508-CFTR processing. However, one homozygous ΔF/ΔF mouse in a 129*FVB background did show a response to forskolin in the normal range using gallbladder (Fig. 7 *A*) and ileum (not shown). Therefore, more complex relationships involving several genetic loci can not yet be excluded and require further study.
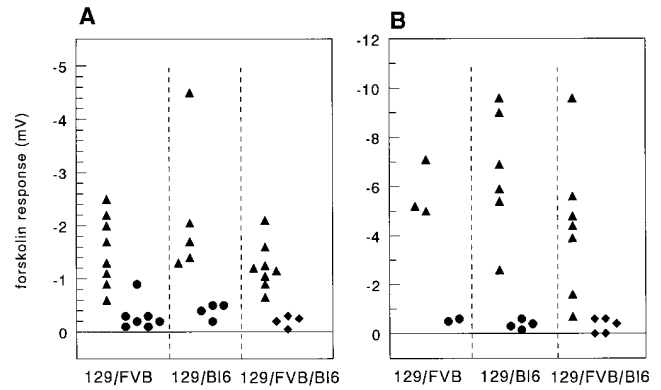
Figure 7. Forskolin responses in homozygous ΔF/ΔF mice gallbladder and caecum in mice strains with different genetic backgrounds. Gallbladder (*A*) and caecum (*B*) of mice from ΔF508 CFTR strains with different genetic backgrounds were mounted in the Ussing chamber and monitored for their electrical response to forskolin (ΔPD, mV). 129/FVB and 129/Bl6 were obtained by blastocyst injection and crossing into FVB and C57BL/6 type animals. 129/FVB/Bl6 was obtained by crossing ΔF/+ (129/FVB) with +/− cftr[m1cam] (129/C57BL6). (▲) +/+, +/Δ and +/− mice; (●) ΔF/ΔF mice; (◆) ΔF/− mice.

Discussion

CFTR mRNA expression is normal in mutant mice. Using the "hit and run" procedure, we have generated a ΔF508-CFTR mouse model without modifying the intron structure of the CFTR gene (14). Our quantitative PCR data show that in heterozygotes the expression levels of normal and mutant alleles are comparable in intestine and salivary gland. Also in homozygote normal and mutant mice the expression levels are not significantly different. In two other ΔF508-CFTR mouse models created by homologous recombination, low CFTR mRNA levels were reported in salivary glands and intestine (15, 16). In these models an expression cassette encoding a selectable marker was introduced into the flanking intron, in addition to the ΔF508 mutation in exon 10. Comparison with our data suggests that the presence of this transcription unit affects the CFTR mRNA levels by interfering with RNA polymerase activity or RNA processing.

Maturation of mouse ΔF508-CFTR is abnormal. Immunochemical analysis of CFTR expression in intact mouse tissues is difficult with the available antisera. This can be attributed in part to relatively low expression levels as in gallbladder tissue (17*a*) and to proteolytic activity, especially in intestinal tissue (H.R. de Jonge, unpublished data). This limits the scope of our investigations to tissues that give consistent and reproducible data. We were able to make reproducible western blots of total oviducts from normal and mutant mice with a purified antibody raised against the carboxy terminus of rodent CFTR (Fig. 2). The data show that CFTR antigen is produced in both normal (+/+) and mutant (ΔF/ΔF) mice, but not in CFTR deficient (−/−) mice. However, the proportion of mature, fully glycosylated CFTR is severely reduced in homozygous mutant. We conclude that the ΔF508 mutation in the mouse CFTR protein results in a processing defect similar to that observed with human ΔF508-CFTR. The available evidence suggests that transfer to the Golgi system and subsequent full glycosylation of the human mutant protein does not occur, because proper chaper-

onin-dependent folding is arrested in the endoplasmic reticulum (7, 8, 10). With the same antibody as used for western blot analysis, we could show specific staining of the apical region of normal mouse jejunum crypt epithelial cells (Fig. 3, *A, B, E,* and *F*). Specificity of the staining was verified with serum pre-absorbed with the antigenic peptide (not shown) and jejunum of CFTR-deficient mice (Fig. 3, *C* and *D*). This is in agreement with localization studies in human intestine (20) and rat (24). In jejunum crypts of mice homozygous for the ΔF508 mutation we did not observe a preferential staining of the apical region. Most crypts seemed devoid of specific staining. However, with this method we cannot rule out that cytoplasmic CFTR is present (note that also in control cells no specific cytoplasmic staining above background can be seen Fig. 3). In several preparations some crypts did stain more intensely than background but the signal was not concentrated to the apical region as in normal crypts. These observations are in agreement with a processing defect of mouse ΔF508-CFTR that prevents translocation of the protein to the apical region.

Temperature dependent apical targeting of ΔF508-CFTR. Airway cells of ΔF508 mutant mice in primary culture have increased cAMP-induced chloride conductance when cultured at reduced temperature (16). We were unable to detect CFTR chloride channel activity in primary airway cells using patch clamp single channel analysis (P.J. French, unpublished data). In contrast, cultured mouse gall bladder cells provide a convenient system for the study of CFTR with this method. This allowed us to show that the actual frequency of active mutant CFTR molecules at the plasma membrane is increased by incubation of the gallbladder cells at low temperature. In homozygous mutant cells cultured at 37°C few CFTR channels were observed, i.e., 1% of the normal level at this temperature (Fig. 6). The expression of ΔF508-CFTR channels increased to 16% of normal levels when cells from homozygous mutants were grown at 27°C (Fig. 6). A similar behavior was observed with human ΔF508-CFTR (10).

Channel activity of ΔF508-CFTR. The channel conductance and anion selectivity of mouse ΔF508-CFTR is in our analysis indistinguishable from normal mouse CFTR (Fig. 4). In addition, the open probability (Po) and number of closing events during a burst of activity of ΔF508-CFTR are normal. Studies of human ΔF508-CFTR are inconsistent at this point as two groups reported normal conductance but reduced Po for human ΔF508-CFTR (10, 11) whereas others claimed a normal conductance and Po (25). Since the activity of the CFTR chloride channel depends on a number of parameters in particular the state of phosphorylation of the protein, the reported difference in relative Po may result from differences in experimental conditions.

Residual activity of ΔF508-CFTR. Both Ussing chamber experiments (14) (Fig. 7), and patch clamp analysis (Fig. 6) in our model indicated a low but significant level of apical activity of mouse ΔF508-CFTR at physiological temperature. This is confirmed by the western blot analysis (Fig. 2), which shows a low level of fully glycosylated CFTR. Interestingly, a minority of human ΔF508 CFTR homozygotes possess a small residual intestinal chloride permeability, which correlates with a relatively mild clinical status (21). Unpublished data showed that in some, but not all, cases this activity is insensitive to the channel blocker DIDS (H. Veeze, personal communications). This would suggest that in these cases the residual activity is due to ΔF508-CFTR. It is possible therefore, that a significant level of

correct processing is also present in a subgroup of human ΔF508 CFTR homozygotes. Immunocytochemical analysis of airway cells from ΔF508 CFTR patients seem to confirm this (26). It will be of great interest to analyze the genetic and environmental factors which contribute to this phenomenon. Our current data indicate that the level of mutant CFTR activity, as determined by Ussing chamber experiments, is quite constant in the different genetic backgrounds tested (Fig. 7). The one exception to this rule we found sofar is intriguing, but extensive further studies are required to establish a genetic basis for this effect. The level of ΔF508-CFTR processing could differ in various tissues and small variations in apical activity levels could have profound effects on pathology. Our electrophysiological data, supported by immunochemical data, show that in all epithelial tissues studied sofar the ΔF508 mice have severely reduced apical activity. However, a careful analysis of ΔF508-CFTR processing kinetics may reveal subtle differences between cell types.

Applications of the ΔF508 mouse model. Our data show that the tissues of the ΔF508 mouse model provide a valid model for the processing defect of the human ΔF508-CFTR mutation. It gives us the opportunity to study several aspects of CFTR function in more detail in intact tissues. CFTR is active in intracellular compartments (9), possibly affecting the pH of vesicular compartments. This could explain why CFTR deficient cells produce mucins and surface glycoproteins with abnormal carbohydrate structures (27–31). These abnormalities may contribute to the formation of abnormal secretions and to the reduced clearance of airway pathogens characteristic of CF. CFTR is involved in regulated endocytosis and exocytosis in some cell types (32, 33). In addition, recent evidence suggests that CFTR either directly or indirectly interacts with other ion transport systems (34, 35). ΔF508-CFTR expressed in epithelial cells may be partially active in these processes. Therefore, we may expect to observe differences between ΔF508 mice and mice with complete loss of function mutations (knockout). It will be interesting to compare ΔF508 mice with knockout mice in an experiment in which the mice are challenged with lung pathogens (36). Furthermore, the ΔF508 mouse model will allow us to study conditions that may enhance the activity of ΔF508-CFTR at the apical epithelial membrane in vitro and in vivo. Processing of normal CFTR involves chaperonin mediated folding and core glycosylation at the endoplasmic reticulum. This is followed by full glycosylation in the Golgi system and transport to the apical membrane. It is a rather inefficient process since approximately 75% of normal CFTR is degraded in immature form by cellular proteases (7, 8). Processing of ΔF508-CFTR to a fully glycosylated apical form is severely reduced. The striking stimulating effect of reduced temperature on ΔF508-CFTR expression, both with human and mouse mutants, suggests that the processing block can be relieved within the range of physiological conditions. We can consider several approaches towards finding therapeutic substances. Compounds which interfere with ΔF508-CFTR-chaperonin interaction may improve processing by relaxing the quality control mechanism. An example of this may be glycerol, which has an effect comparable to low temperature (37). Inhibition of CFTR degradation may improve processing of mutant CFTR, although this approach has not been successful to date (7). CFTR at the plasma membrane is activated by ATP binding and multi-site phosphorylation of the large cytoplasmic regulatory domain (3, 38). Therefore, substances that stabilize the

open state of CFTR (39, 40) or inhibit protein phosphatases (41–43) are expected to improve the activity of both normal and ΔF508-CFTR. These studies may lead to new developments, not only in our understanding of membrane protein processing, but also towards effective therapies for CF.

Acknowledgments

References

1. Boat, T., M.J. Welsh, and A. Beaudet. 1989. Cystic Fibrosis. *In* Metabolic Basis of Inherited Disease. C. Scriver, A. Beaudet, W. Sly, and D. Valle, editors. McGraw Hill, New York. 2649–2860.

2. Welsh, M.J. 1994. The path of discovery in understanding the biology of cystic fibrosis and approaches to therapy. *Am. J. Gastroenterol.* 89 (8):S97–S105.

3. Riordan, J.R. 1993. The cystic fibrosis transmembrane conductance regulator. *Ann. Rev. Physiol.* 55:609–630.

4. Kerem, B.S., J.M. Rommens, J.A. Buchanan, D. Markiewicz, T.K. Cox, A. Chakravarti, M. Buchwald, and L.C. Tsui. 1989. Identification of the cystic fibrosis gene — genetic analysis. *Science (Wash. DC).* 245:1073–1080.

5. Cheng, S.H., R.J. Gregory, J. Marshall, S. Paul, D. W. Souza, G.A. White, J. R. Riordan, and A.E. Smith. 1990. Defective intracellular transport and processing of CFTR is the basis of most cystic fibrosis. *Cell.* 63:827–834.

6. Gregory, R.J., D.P. Rich, S.H. Cheng, D.W. Souza, S. Paul, P. Manavalan, M. P. Anderson, M.J. Welsh, and A.E. Smith. 1991. Maturation and function of cystic fibrosis transmembrane conductance regulator variants bearing mutations in putative nucleotide-binding domain-1 and domain-2. *Mol. Cell. Biol.* 11:3886–3893.

7. Jensen, T.J., M.A. Loo, S. Pind, D.B. Williams, A.L. Goldberg, and J.R. Riordan. 1995. Multiple proteolytic systems including the proteasome, contribute to CFTR processing. *Cell.* 83:129–135.

8. Ward, C.L., S. Omura, and R.R. Kopito. 1995. Degradation of CFTR by the ubiquitin-proteasome pathway. *Cell.* 83:121–127.

9. Pasyk, A.E., and J.K. Foskett. 1995. Mutant (ΔF508) CFTR Cl channel is functional when retained in endoplasmic reticulum of mammalian cells. *J. Biol. Chem.* 270:12347–12350.

10. Denning, G.M., M.P. Anderson, J.F. Amara, J. Marshall, A.E. Smith, and M.J. Welsh. 1992. Processing of mutant cystic fibrosis transmembrane conductance regulator is temperature-sensitive. *Nature (Lond.).* 358:761–764.

11. Dalemans, W., P. Barbry, G. Champigny, S. Jallat, K. Dott, D. Dreyer, R.G. Crystal, A. Pavirani, J.P. Lecocq, and M. Lazdunski. 1991. Altered chloride ion channel kinetics associated with the ΔF508 Cystic Fibrosis mutation. *Nature (Lond.).* 354:526–528.

12. Li, C.H., M. Ramjeesingh, E. Reyes, T. Jensen, X.B. Chang, J.M. Rommens, and C.E. Bear. 1993. The cystic fibrosis mutation (ΔF508) does not influence the chloride channel activity of CFTR. *Nat. Genet.* 3:311–316.

13. Drumm, M.L., D.J. Wilkinson, L.S. Smit, R.T. Worrell, T.V. Strong, R.A. Frizzell, D.C. Dawson, and F.S. Collins. 1991. Chloride conductance expressed by ΔF508 and other mutant CFTRs in xenopus oocytes. *Science (Wash. DC).* 254 (5039):1797–1799.

14. Van Doorninck, J.H., P.J. French, E. Verbeek, R.P.C. Peters, H. Morreau, J. Bijman, and B.J. Scholte. 1995. A mouse model for the cystic fibrosis ΔF508 mutation. *EMBO (Eur. Mol. Biol. Organ.) J.* 14:4403–4411.

15. Zeiher, B.G., E. Eichwald, J. Zabner, J.J. Smith, A.P. Puga, P.B. McCray, M.R. Capecchi, M.J. Welsh, and K.R. Thomas. 1995. A mouse model for the ΔF508 allele of cystic fibrosis. *J. Clin. Invest.* 96:2051–2064.

16. Colledge, W.H., B.S. Abella, K.W. Southern, R. Ratcliff, C. Jiang, S.H. Cheng, L.J. MacVinish, J.R. Anderson, A.W. Cuthbert, and M.J. Evans. 1995. Generation and characterisation of a ΔF508 cystic fibrosis mouse model. *Nat. Genet.* 10:445–452.

17. Ratcliff, R., M.J. Evans, A.W. Cuthbert, L.J. Macvinish, D. Foster, J.R. Anderson, and W.H. Colledge. 1993. Production of a severe cystic fibrosis mutation in mice by gene targeting. *Nat. Genet.* 4 :35–41.

17a. Peters, R.P.C., J.H. van Doornick, P.J. French, R. Ratcliff, M.J. Evans, W.H. Collins, J. Bijman, and B.J. Scholte. 1996. Cystic fibrosis transmembrane conductance regulator mediates the cAMP induced fluid secretion but not the inhibition of resorption in mouse gallbladder epithelium. *Hepatology.* In Press.

18. Bremer, S., T. Hoof, M. Wilke, R. Busche, B. Scholte, J.R. Riordan, G. Maass, and B. Tummler. 1992. Quantitative expression patterns of multidrug-resistance P-glycoprotein (MDR1) and differentially spliced cystic-fibrosis transmembrane-conductance regulator messenger RNA transcripts in human epithelia. *Eur. J. Biochem.* 206:137–149.

19. Kansen, M., R.B. Bajnath, J.A. Groot, H.R. De Jonge, B. Scholte, A.T. Hoogeveen, and J. Bijman. 1993. Regulation of chloride channels in the human colon carcinoma cell line HT29.cl19A. *Pflugers Arch. Eur. J. Physiol.* 422:539–545.

20. Crawford, I., P.C. Maloney, P.L. Zeitlin, W.B. Guggino, S.C. Hyde, H. Turley, K.C. Gatter, A. Harris, and C.F. Higgins. 1991. Immunocytochemical localization of the Cystic Fibrosis gene product CFTR. *Proc. Natl. Acad. Sci. USA.* 88:9262–9266.

21. Veeze, H.J., D.J. Halley, J. Bijman, J.C. De Jongste, H.R. De Jonge, and M. Sinaasappel. 1994. Detection of mild clinical symptoms in cystic fibrosis patients. Residual chloride secretion measured in rectal biopsies in relationship to the genotype. *J. Clin. Invest.* 93:461–466.

22. Puchelle, E., D. Gaillard, D. Ploton, J. Hinnrasky, C. Fuchey, M.C. Bouterin, J. Jacquot, D. Dreyer, A. Pavirani, and W. Dalemans. 1992. Differential localization of the cystic fibrosis transmembrane conductance regulator in normal and cystic fibrosis airway epithelium. *Am. J. Resp. Cell Molec. Biol.* 7:485–491.

23. Dalemans, W., J. Hinnrasky, P. Slos, D. Dreyer, C. Fuchey, A. Pavirani, and E. Puchelle. 1992. Immunocytochemical analysis reveals differences between the subcellular localization of normal and delta-Phe508 recombinant cystic fibrosis transmembrane conductance regulator. *Exp.Cell Res.* 201 :235–240.

24. Ameen, N.A., T. Ardito, M. Kashgarian, and C.R. Marino. 1995. A unique subset of rat and human intestinal villus cells express the cystic fibrosis transmembrane conductance regulator. *Gastroenterol.* 108:1016–23.

25. Li, C., M. Ramjeesigh, E. Reyes, T. Jensen, X. Chang, J.M. Rommens, and C.E. Bear. 1993. The cystic fibrosis mutation (ΔF508) does not influence the chloride channel activity of CFTR. *Nat. Genet.* 3:311–316.

26. Dupuit, F., N. Kalin, S. Brezillon, J. Hinnrasky, B. Tummler, and E. Puchelle. 1995. CFTR and differentiation markers expression in non-CF and ΔF508 homozygous CF nasal epithelium. *J. Clin. Invest.* 96:1601–1611.

27. Carnoy, C., R. Ramphal, A. Scharfman, J. Lo-Guidice, N. Houdret, A. Klein, C. Galabert, G. Lamblin, and P. Roussel. 1993. Altered carbohydrate composition of salivary mucins from patients with cystic fibrosis and the adhesion of Pseudomonas aeruginosa. *Am. J. Respir. Cell Mol. Biol.* 9:323–334.

28. Lo-Guidice, J., J. Wieruszeski, J. Lemoine, A. Verbert, P. Roussel, and G. Lamblin. 1994. Sialylation and sulfation of the carbohydrate chains in respiratory mucins from a patient with cystic fibrosis. *J. Biol. Chem.* 269:18794–18813.

29. Dosanjh, A., W. Lencer, D. Brown, D.A. Ausiello, and J.L. Stow. 1994. Heterologous expression of ΔF508 CFTR results in decreased sialylation of membrane glycoconjugates. *Am. J. Physiol.* 266:C360–366.

30. Cheng, P.W., T.F. Boat, K. Cranfill, J.R. Yankaskas, and R.C. Boucher. 1989. Increased sulfation of glycoconjugates by cultured nasal epithelial cells from patients with Cystic Fibrosis. *J. Clin. Invest.* 84:68–72.

31. Zhang, Y., B. Doranz, J.R. Yankaskas, and J.F. Engelhardt. 1995. Genotypic analysis of respiratory mucous sulfation defects in cystic fibrosis. *J. Clin. Invest.* 96:2997–3004.

32. Bradbury, N.A., T. Jilling, G. Berta, E.J. Sorscher, R.J. Bridges, and K.L. Kirk. 1992. Regulation of plasma membrane recycling by CFTR. *Science (Wash. DC).* 256:530–532.

33. Prince, L.S., R.B. Workman, and R.B. Marchase. 1994. Rapid endocytosis of the cystic fibrosis transmembrane conductance regulator chloride channel. *Proc. Natl. Acad. Sci. USA.* 91:5192–5196.

34. Schwiebert, E.M., M.E. Egan, T. Hwang, S.B. Fulmer, S.S. Allen, G.R. Cutting, and W.B. Guggino. 1995. CFTR regulates outwardly rectifying chloride channels through an autocrine mechanism involving ATP. *Cell.* 81:1063–1073.

35. Stutts, M.J., C. M. Canessa, J.C. Olsen, M. Hamrick, J.A. Cohn, B.C. Rossier, and R.C. Boucher. 1995. CFTR as a cAMP-dependent regulator of sodium channels. *Science (Wash. DC).* 269:847–850.

36. Mills, C.L., J.R. Dorin, D.J. Davidson, D.J. Porteus, E.W.F. W. Alton, R.L. Dormer, and M.A. Mcpherson. 1995. Decreased beta-adrenergic stimulation of glycoprotein secretion in CF mice submandibular glands: reversal by the methylxanthine, IBMX. *Biochem. Biophys. Res. Comm.* 215:674–681.

37. Sato, S., Ward, C.L., Krouse, M.E., Wine, J.J., and R.R. Kopito. 1996. Glycerol reverses the misfolding phenotype of the most common cystic fibrosis mutation. *J. Biol. Chem.* 271:635–638.

38. Gadsby, D.C., and A.C. Nairn. 1994. Regulation of CFTR channel gating. *Trends Biochem. Sci.* 19:513–518.

39. Hwang, T.C., G. Nagel, A.C. Nairn, and D.C. Gadzby. 1994. Regulation of the gating of CFTR Cl channels by phosphorylation and ATP analysis. *Proc. Natl. Acad. Sci. USA.* 91:4698–4702.

40. Gribkoff, V.K., G. Champigny, P. Barbry, S.I. Dworetzky, N.A. Meanwell, and M. Lazdunski. 1994. The substituted benzimidazole NS004 is an opener of the cystic fibrosis channel. *J. Biol. Chem.* 269:10983–10986.

41. Hanrahan, J.W., F. Becq, J.H. Tabcharani, T.J. Jensen, X.B. Cheng, and J.R. Riordan. 1995. Use of phosphatase inhibitors as therapeutic agents to activate mutant CFTR. *Ped. Pulmonol.* suppl 12:152–153.

42. De Jonge, H.R., A.G.M. Bot, P.J. French, J. Bijman, M. Sinaasappel, and H.J. Veeze. 1995. Synergistic activation of ΔF508-CFTR Cl-channels by cyclic AMP agonists and the tyrosine kinase inhibitor genistein. *Ped. Pulmonol.* suppl 12:186.

43. Becq, F., T.J. Jensen, X.B. Chang, A. Savoia, J.M. Rommens, L.C. Tsui, M. Buchwald, J.R. Riordan, and J.W. Hanrahan. 1994. Phosphatase inhibitors activate normal and defective CFTR chloride channels. *Proc. Natl. Acad. Sci. USA.* 91:9160–9164.